Fractal quantum well heterostructures for broadband light emitters

M. Hagerott Crawford, P. L. Gourley, K. E. Meissner, M. B. Sinclair, E. D. Jones, W. W. Chow and R. P. Schneider, Jr.

Sandia National Laboratories, Albuquerque, NM 87185-0350

ABSTRACT

We examine carrier relaxation and radiative recombination in AlGaAs based near IR and AlGaInP based visible fractal quantum well heterostructures. Through temperature dependent photoluminescence, we demonstrate that enhanced population of higher lying energy levels can be achieved by varying the thickness of the layers in the fractal heterostructure. This distribution of carriers results in room temperature emission over a relatively broad range of wavelengths: approximately 700-855 nm for AlGaAs structures and 575-650 nm for AlGaInP structures. Spectra are compared to theoretical calculations to evaluate the non-equilibrium nature of the carrier distributions. Time resolved photoluminescence measurements demonstrate an approximately linear relationship between the radiative decay time and the layer thickness of the structure. Correspondingly, integrated luminescence measurements at room temperature reveal a factor of four increase in the light output efficiency of the structure as the fractal layer thickness is increased from 50 Å to 400 Å. The applicability of these heterostructures to broadband LEDs is discussed.

key words: light emitting diodes, quantum well heterostructures, broadband light sources

1. INTRODUCTION

The ability to combine the high optical efficiency that is intrinsic to semiconductor photonic materials with broadband spectral emission is desirable for a number of technologies. In particular, the short coherence length of broadband LEDs leads to reduced Rayleigh scattering and improved noise performance in fiber optic gyroscopes[1] as well as improved spatial resolution in optical time domain reflectometry. Broadband LEDs are also well suited for wavelength-multiplexing-based fiber optical networks and more generally as a compact light source for spectroscopic measurements in the analytical chemistry and medical fields. Visible broadband LEDs in particular offer great potential for illumination applications. Semiconductor based broadband LEDs offer many advantages over conventional tungsten and fluorescent bulbs, including a substantially higher electrical to optical power conversion efficiency, compact and rugged packaging as well as increased operating lifetime.

In recent years, there has been a substantial amount of research devoted to the development of high power broadband LEDs, particularly in the near IR region of the spectrum[2-8]. One of the most successful designs to enable high power LEDs is that of a superluminescent diode (SLD) in which loss is introduced into the cavity of an edge emitting laser diode through antireflection coatings, an absorbing region or a bent waveguide configuration in order to inhibit lasing and thus allow the increase of amplified spontaneous emission with high levels of injected current. To increase the spectral width of emission, several heterostructure designs have been employed. The majority of the designs take advantage of the fact that the gain spectrum of the quantum well heterostructure is broader than that of a bulk double heterostructure for a given injected current density due to the higher carrier densities in the quantum well and the smaller density of states at a given energy[5].

DISCLAIMER

DISCLAIMER

Portions of this document may be illegible in electronic image products. Images are produced from the best available original document.

Using a single quantum well heterostructure in a SLD geometry, one can obtain emission from both the n=1 and n=2 confined transitions through gain saturation and thus achieve a substantially broader emission spectrum than from a non-SLD geometry. J. Mantz, et. al[2] have reported a 100 Å GaAs single quantum well SLD structure with 95 nm spectral bandwidth centered at 820 nm and producing 3.2 mW at a 200 mA drive current. To achieve a more uniform spectral output, an asymmetric multiquantum well design has been employed[3] which consists of two AlGaAs quantum wells of properly designed well width and composition to yield similar gain properties for the n=1 transitions in both wells. This approach has yielded SLDs with greater than 100 nm spectral bandwidth centered at 820 nm and 2.1 mW output power at 250 mA drive current. Moseley, et. al.[4] has employed an AlGaAs multiple quantum well active region with up to ten quantum wells of different Al concentration to yield greater than 144 nm spectral bandwidth centered at 750 nm. Similar designs have been employed in InGaAs/ InGaAsP based LEDs for broadband emission at 1.5 microns[6-8]. To date, relatively little has been published on applying these designs to visible semiconductor materials. In one report, Semenov et. al.[9] demonstrated 12 nm spectral bandwidth and spectral ripple less than 10% from SLDs employing a 0.1 μm thick AlGaInP active region. The devices produced up to 4 mW output power centered at 670 nm.

An entirely different heterostructure design based on a fractal sequence of quantum wells has been recently proposed by P. L. Gourley et. al.[10] as a possible means of generating broadband emission. These structures consist of multiple layers of AlGaAs alloys in which the bandgaps are designed to vary in a fractal manner throughout the structure. As fractal geometries are readily seen in nature to contribute to the efficient collection of sunlight and distribution of fluids, the semiconductor fractal quantum well heterostructure may offer the potential of controlling the carrier transport and radiative recombination in the material in a manner that is not possible with more conventional geometries. Absorption, photoluminescence and time resolved spectroscopy of these AlGaAs based fractal quantum well heterostructures (FQWHs) demonstrated that both optical and transport properties of the FQWHs are strongly affected by the thickness of the fractal layers. In this paper, we further examine the optical and transport properties of AlGaAs based near IR FQWHs and extend the study to AlGaInP based visible FQWHs. Temperature dependent photoluminescence and time resolved photoluminescence are performed to evaluate the novel physics of FQWHs and to assess their potential as broadband light emitters.

2. HETEROSTRUCTURE DESIGN

Both the AlGaAs based FQWHs and the AlGaInP based FQWHs were grown by MOVPE on GaAs substrates. The general fractal sequence that applies to both materials is formed by the successive replacement of wells and barriers with finer scale quantum wells, as described in reference 10. Starting with a layer of thickness d and energy gap E_g, one then replaces this layer with a three layer sequence consisting of a single quantum well of energy gap E_g- ΔE clad on each side by barriers of energy E_g. This replacement is continued for further generations of the fractal sequence. For the AlGaAs based FQWH, the highest energy gap material is $Al_{0.4}Ga_{0.6}As$ with the lower energy layers consisting of $Al_xGa_{1-x}As$ with x = 0.3, 0.2, 0.1, 0. A schematic of the lowest energy conduction and valence bands for the AlGaAs FQWH is shown in Figure 1. The AlGaInP based visible FQWHs have an identical fractal sequence and contain $(Al_yGa_{1-y})_{0.5}In_{0.5}P$ layers with y = 0.48, 0.36, 0.24, 0.12, 0 .

The layer thickness is kept constant throughout the fractal structure (i.e. only the bandgap varies spatially) and the fractal sequence for both material systems consists of 81 layers in total. Four samples were grown for each material system, with characteristic layer thickness of 50 Å, 100 Å, 200 Å and 400 Å, yielding a total active region thickness of 4050 Å, 8100 Å, 1.62 μm and 3.24 μm for the four structures. Throughout this discussion, the different FQWHs will be identified by the characteristic thickness of each of the layers in the structure. The wells for both

material systems were intentionally grown without strain to reduce the probability of defect formation in these relatively thick structures.

3. EXPERIMENTAL DATA AND ANALYSIS

3.1 Temperature dependent photoluminescence

3.1.1 Experimental data

One aspect of this particular FQWH design that lends itself readily to broadband emission is the large number of confined energy levels that are present in the complex structure as well as the systematic increase in the number of wells composed of higher bandgap alloys. We have performed temperature dependent photoluminescence on both sets of FQWHs in order to more clearly identify the dominant radiative transitions and to evaluate the thermally driven carrier relaxation to the lowest energy branch of the fractal structure as a function of layer thickness. The excitation source was a continuous wave Argon laser at 514.5 nm. The excitation power ranged between 1mW and 50 mW for the AlGaAs samples (the higher power used at higher temperatures for a better signal to noise ratio) and between 0.1mW and 2 mW for the AlGaInP samples. The sample was placed in a low temperature cryostat and the laser light was delivered to the sample by means of an optical fiber with 100 μm core diameter. These excitation conditions result in an absorbed carrier density of approximately 10^{14}- 10^{16} cm^{-3}. A SPEX (model 1401) monochrometer was used with a Hamamatsu R3310-2 photon counting photomultiplier tube. The resolution of the system was greater than 0.5 meV. A careful measurement of the spectrally dependent system response was performed to ensure that the relative ratios of the spectral peaks are valid.

In Figure 2a we show the photoluminescence spectrum and the log of the spectrum from the 50 Å AlGaAs FQWH. The topmost segment of the figure displays the spectrum at 1.4 K where we see that the spectrum is dominated by five peaks covering the energy range of 1.51-1.85 eV. The lowest energy peak is attributed to the GaAs substrate. A simple finite square well calculation[11] predicts an n=1 transition from the GaAs well of approximately 1.569 eV. The spectrum shows a peak at 1.574 eV, in reasonable agreement with the predicted energy. Beyond this energy level, the identification of the transitions is more difficult. The finite square well model predicts an n=1 transition from an $Al_{0.1}Ga_{0.9}As$ well with $Al_{0.2}Ga_{0.8}As$ barriers at approximately 1.700 eV as well as an n=1 transition at 1.82 meV for $Al_{0.2}Ga_{0.8}As$ wells with $Al_{0.3}Ga_{0.7}As$ barriers. The data is roughly in agreement with these energies, with transitions seen at 1.712 eV and 1.832 eV, however the nature of the transition at 1.590 eV is not clear. Furthermore, the peak at 1.712 eV does not demonstrate a significant energy shift for the samples with greater quantum well width and therefore may be arising from a transition in the higher energy region of the center branch of the fractal structure where the "well" thickness is already rather large.

As we increase the temperature of the sample, we see that the emission from the higher energy levels is strongly decreased. By 200 K, the emission is reduced to primarily the GaAs substrate and the GaAs quantum well contributions, with a full width half maximum (FWHM) spectral linewidth of only 30 meV. A significantly broader spectum has been seen from a similar structure with 100 Å layer thickness, as seen in Figure 2b. The spectum at low temperature is similar to that of the 50 Å layer thickness sample, however contributions from the higher energy levels are maintained up to 200 K. Although the emission shows a significant spectral modulation, it covers the range of 1.49-1.70 eV. In Figure 2c we show the temperature dependent photoluminescence for an AlGaAs FQWH with 200 Å layer thickness. This structure shows further enhancement of the higher energy emission as compared to the 100 Å structure, with emission over the 1.48-1.78 eV (700-840 nm) range. The relatively small intensity of emission

from the substrate and GaAs quantum well may be due to the increased thickness of the structure relative to the absorption depth of the incident laser beam.

Insight into the non-equilibrium nature of the carrier distributions can be gained by examination of the log plots of the emission spectra. For example, we see from the slopes of the (log) peaks for 50 Å FQWH at 100 K that the carrier distributions in each branch appear to be thermalized with the lattice. However, the fractal branch-to-branch distribution does not appear to be thermalized with the lattice, as seen by the slope of the entire spectral distribution (relative peak intensities) and indicates an effective temperature that is considerably greater than the lattice. At high temperatures, we see that the 50 Å FQWH spectrum indicates a branch-to-branch carrier distribution that is nearly in equilibrium with the lattice, whereas the 100 Å and 200 Å FQWHs still demonstrate a substantially higher effective temperature for the branch-to branch carrier distribution. As a final comparison, we show the room temperature photoluminescence for the three samples in Figure 3a.

Several aspects of the FQW design contribute to the broader spectral output for the structures with thicker layers. In general, the fractal design incorporates local minima at higher energy which trap carriers and inhibit further energy relaxation. As shown in Figure 3a, the effectiveness of these local minima in trapping carriers and allowing for subsequent recombination at higher energy is directly related to the thickness of the barrier layers. While the fractal design also enables a large number of energy levels, it appears that generally it is the lowest energy levels in each branch that contribute to the emission spectrum.

Similar photoluminescence experiments were performed on the AlGaInP based visible FQWH samples. The incident laser power was kept low to avoid heating effects, and ranged between 0.1 mW and 2 mW. The low temperature spectra consist of three dominant peaks, each of which show shifts due to quantum confinement effects. In Figure 3b we show a comparison of the room temperature emission for FQWHs with 50 Å, 100Å and 200 Å characteristic layer thicknesses. The 200 Å AlGaInP FQWH demonstrates the largest spectral width, with emission over the 1.93-2.15 eV (575-650 nm) range. In comparison, the 200 Å AlGaAs FQWH (Figure 3a) demonstrates room temperature emission over the 1.45-1.75 eV (855-700 nm) range.

3.1.2 Theoretical modeling

Given the complexity of the fractal heterostructure, it is difficult to properly model the carrier transport and radiative recombination. While a more complete model is being developed based on a rate equation description[12], we present here a simple model to evaluate the non-equilibrium nature of the carrier populations in the branches of the fractal heterostructure at each temperature. As our temperature dependent photoluminescence experiments suggest that the dominant transitions arise from the lowest confined energy level of three branches of the fractal structure, we consider a system with quantum wells at three transition energies as a simplified version of our structure We also make the assumption that each of the wells at a given energy gap have the same carrier density. This assumption is not entirely accurate due to the fact that the optical pumping geometry yields higher carrier densities at the top of the structure, however, we consider it to be a reasonable approach for this simple model. At present, we have confined our calculations to the 100 Å AlGaInP FQW structure.

Beginning with Luttinger theory[13], we calculate the bandstructure and effective masses for each of the quantum wells. The maximum total number of carriers in the system is estimated by the absorbed photon flux, assuming an internal quantum efficiency of 1. Given the low incident Argon laser power of 0.1 mW and the 10^{-8} cm^2 excitation area (constant for each temperature), we estimate the total carrier density in the system to be less than or equal to 10^{14} cm^{-3}. With the carrier densities in each well as an input parameter, the effective fermi levels in each well are determined by[13]

$$\beta\mu_\alpha = \ln\,[\exp(\pi\beta\hbar^2 Nd/m_\alpha) - 1] \qquad (1)$$

where $\beta = kT$, d is the quantum well thickness, N is the carrier density, and m_α is the effective mass for electrons or holes. The spontaneous emission is calculated by integrating the product of the electron and hole probability distributions over k-space and multiplying the resultant curves by the number of identical wells in the fractal structure. In order to maintain some consistency with the experimental data, we have to take into account the reduced quantum efficiency of the material at elevated temperature. We do this by normalizing the total carrier density by the integrated emission intensity from the sample at each temperature. Although the inclusion of a dephasing time would enable a better approximation of the experimental data, we have not included it in these calculations.

In Figure 4, we show the experimentally determined photoluminescence spectrum of the 100 Å AlGaInP FQWH at 100 K (solid line) with the theoretical calculations (dashed line). The relative intensity ratio between the three peaks is well approximated assuming a carrier concentration of $1.78\text{x}10^{13}$ cm^{-3} in the lowest energy well, $1.25\text{x}10^{13}$ cm^{-3} in each of the four wells at the next highest energy gap and $0.18\text{x}10^{13}$ cm^{-3} in each of the four wells of the third highest energy gap. Given these carrier concentrations, an effective Fermi level (measured with respect to the bandgap of the given well) for the electrons (holes) is -0.072 eV (-0.088 eV) for the first well, -0.075 eV (-0.091 eV) for the each of the next highest energy gap wells and -0.092 eV (-0.108 eV) for each of the wells with the third highest energy gap.

Similar fits were performed on the photoluminescence data for each temperature and effective Fermi levels were determined for the electrons and holes. In Figure 5, we show a schematic of the position of the electron effective Fermi levels for a selection of temperatures. A schematic of the fractal lowest energy conduction band is shown on the left hand side of the figure while the simplified structure assumed in the model is shown on the right hand side of the figure. At a low temperature of 2.3 K, the effective Fermi levels for the three wells are well separated and just below the n = 1 confined level at 14 meV above the bandgap. The reduction in radiative efficiency of the material with increasing temperature results in the reduction in the effective Fermi level energy for a given well as the temperature is increased, as shown in Figure 5.

As the temperature increases, the separation between the electron effective Fermi levels decreases, most noticeably for the second and third well. At a temperature of 200 K, the population in the third well has significantly dropped such that the effective Fermi level is roughly coincident in energy with that of the second well. The fact that the first and second well still have a reasonable separation in effective Fermi levels suggests that the entire system is not yet in thermal equilibrium, however, the emission bandwidth has been reduced due to the inability of the structure to maintain a large number of carriers in the third well. In general, these calculations give us a semi-quantitative indication of how well our fractal structures can maintain a non-equilibrium distribution of carriers to enhance emission from higher energy levels. As seen from these calculations and reflected in the room temperature photoluminescence spectra in Figure 3b, the 100 Å AlGaInP FQWH is marginally successful at maintaining a non-equilibrium distribution of carriers at elevated temperatures.

3.2 Time resolved photoluminescence experiments.

Another interesting consequence of the fractal design is the potential ability to control the radiative lifetimes of the system with varying fractal layer thickness. In order to explore this potential more fully, we have performed time resolved photoluminescence experiments on the AlGaInP-based visible FQWHs. The excitation source in the experiments was a frequency doubled Ti: sapphire laser with a pulse width of approximately 150 fsec. The 3.1 eV (400 nm) excitation energy is significantly above highest bandgap alloy ($(Al_yGa_{1-y})_{0.5}In_{0.5}P$ with y = 0.48,

Eg = 2.19 eV[14]) in the system. The average power of excitation was approximately 40 mW and the beam was focused to a relatively small 10 μm diameter spot size. It should be noted that this results in a very high excitation density (approximately 10^{20} cm^{-3}) and therefore is a different regime that of the temperature dependent photoluminescence experiments. The primary reason for using these high excitation conditions was to obtain signals with a reasonable signal to noise ratio. The spectrally integrated luminescence was directed into a Hamamatsu streak camera with a 2-dimensional thermoelectrically cooled CCD detector. The time resolution of the system is approximately 20 psec. The experiments were performed at room temperature.

In Figure 5, we show the time decay of the integrated emission spectra for AlGaInP FQWHs with 50 Å, 100 Å, 200 Å and 400Å layer thickness. Despite the fact that we are not spectrally resolving the contributions from the individual wells, we see that the emission decays approximately as a single exponential for the 50 Å, 100 Å and 400 Å FQWHs. The 200 Å FQWH gives an indication of a two component decay with an initially fast decay time followed by a slower decay time. If we first examine the decay for the 50 Å FQW sample, we see a detection limited risetime of 20 psec and a relatively short decay time of 0.58 nsec. The 100 Å FQWH has a similar risetime and a 1.39 nsec decay time, while the longer component of the 200 Å FQWH decay is approximately 2.34 nsec. In contrast to the other three samples, a significant delay was observed in the onset of the emission from the 400 Å FQWH. This delay may be related to the time needed to accumulate carriers in the lowest energy wells. The decay time of the 400 Å FQWH was measured to be 7.45 nsec.

In the inset of Figure 5, we have plotted the measured decay times as a function of FQWH layer thickness on a log-log scale. The slope of the curve fit is 1.2 , demonstrating a nearly linear relationship between carrier lifetime and fractal layer thickness. As a complementary experiment, we examined the spectrally resolved emission from each of the four AlGaInP-based FQWHs with similar high excitation from the frequency doubled Ti:sapphire laser system. The room temperature spectra are shown in Figure 6. Under these high excitation conditions, the enhanced spectral width of the 400 Å FQWH is clearly seen, with emission spanning the 570-680 nm range. The integrated intensity of the 400 Å FQWH is a factor of four greater than that from the 50 Å FQWH for similar excitation conditions. In the inset of Figure 6, we plot the log of the integrated intensity from each of the FQWHs versus the log of the decay time determined from time resolved photoluminescence experiments. The curve fit demonstrates a sublinear power dependence, with a slope of 0.6.

The longer lifetimes and higher emission efficiencies of the FQWHs with thicker layers may both be explained by the fact that the carriers are less mobile given the thick barrier layers that are present and are less likely to encounter nonradiative recombination sites at the surface or the layer interfaces. One might expect that the nearly linear relationship that has been seen between the luminescence decay time and the layer thickness should result in a linear relationship between the integrated intensity and the decay time. The fact that the 400 Å FQWH yields only a factor of four greater integrated emission than the 50 Å may be due to the slightly reduced material quality of the thicker structure. Although the structures were nominally grown lattice matched, a higher percentage of defects and dislocations were detected as the overall sample thickness was increased. Spectrally resolved time dependent photoluminescence experiments as well as ultrafast transient absorption experiments are in progress to lend further insight into carrier relaxation and recombination in these structures.

4. CONCLUSION

We have performed temperature dependent photoluminescence and time resolved photoluminescence studies on AlGaAs-based near IR and AlGaInP-based visible fractal quantum well structures to evaluate their potential as broadband emitters. Both experimental techniques reveal that important emission properties, including the spectral bandwidth of emission as well as the luminescence decay time, can be significantly enhanced by increasing the fractal layer

thickness. A nearly linear relationship has been established between the fractal layer thickness and the luminescence decay time and room temperature emission spectra of the AlGaInP fractal structures under high excitation conditions reveal a factor of four increase in the light emission efficiency as the layer thickness is increased form 50 Å to 400 Å. The reduced mobility of carriers in the structures with thicker barriers and the subsequent reduction in nonradiative recombination at surface states or layer interfaces is one factor which contributes to these results. Under conditions of very low excitation, the room temperature emission spectra for the FQWHs with 200 Å layer thicknesses cover a wide range of emission wavelengths: 700-855 nm for the near IR structures and 575-650 for the visible structures. While the present designs have not been optimized for spectral uniformity, we are presently designing structures with different alloy compositions that should provide a more uniform output.

The fractal geometry therefore shows strong potential as a source of efficient broadband emission in the near-IR and visible region of the spectrum. In order to implement this heterostructure into an LED active region, carrier injection issues must be addressed. In general, the thickness of the structures described here are too great for efficient electrical injection across the entire structure. While increased fractal layer thickness has been shown to improve light efficiency and spectral bandwidth, it is a detrimental factor to electrical injection efficiency. A compromise must be made between the number of layers needed for multiple energy levels and multilayer barrier designs and the appropriate diffusion lengths of the carriers (especially holes) in the materials. Indeed, the experiments described here were performed with optical excitation such that the electrons and holes are initially generated in the same spatial region of the sample and different behavior may be seen with electrical injection in a p-n junction. In addition, heating should be more severe in an LED than in our optical pumping experiments and this should affect carrier relaxation in the structures. Work is currently in progress to evaluate electrically injected multiquantum well structures and fractal quantum well structures to optimize the spectral bandwidth as well as the spectral uniformity of emission.

5. ACKNOWLEDGMENTS

The authors gratefully acknowledge fruitful discussions with I. J. Fritz and the technical assistance of M. Russell and A. E. McDonald. This work was supported by the Division of Materials Science, Office of Basic Energy Science of the United States Department of Energy under contract DE-AC04-94AL85000.

6. REFERENCES

[1]K. Bohm, P. Marten, K. Petermann and E. Weidel, "Low-drift fibre gyro using a superluminescent diode", Electron. Lett., **17**, pp. 352-353, 1981.

[2]J. Mantz, H. Hager, E. Chan and C. S. Hong, "Single quantum well edge emitting broadband LED", Electron. Lett., **26**, pp. 1807-1808, 1990.

[3]H. Hager, C. S. Hong, J. Mantz, E. Chan, D. Booher and L. Figueroa, "Broad-band emission from a multiple asymmetric quantum-well light-emitting diode", IEEE Photon. Technol. Lett., **3**, pp. 436-438, 1991.

[4]A. J. Moseley, D. J. Robbins, C. Meaton, R. M. Ash, R. Nicklin, P. Bromley, R. R. Bradley, A. C. Carter, C. S. Hong and L. Figueroa, "Broadband GaAs / $Al_XGa_{1-X}As$ Multi-Quantum Well LED", Quantum Optoelectronics, Technical Digest Series, vol. 7, (Optical Society of America, Washington DC), pp. 193-196, 1991.

[5]T. R. Chen, L. Eng, H. Zhuang and A. Yariv, "Quantum well superluminescent diode with very wide emission spectrum", Appl. Phys. Lett., **56**, pp. 1345-1347, 1990.

[6]S. Kondo, H. Yasaka, Y. Noguchi, K. Magari, M. Sugo and O. Mikami, "Very wide spectrum multiquantum well superluminescent diode at 1.5 μm", Electron. Lett., **28**, pp. 132-133, 1992.

[7]Osamu Mikami, Hiroshi Yasaka and Yoshio Noguchi, "Broader spectral width InGaAsP active layer superluminescent diodes", Appl. Phys. Lett., **56**, pp. 987-989, 1990.

[8]Yoshio Noguchi, Hiroshi Yasaka, Osamu Mikami and Haruo Nagai, " High-power, broad-band InGaAsP superluminescent diode emitting at 1.5 μm", J. Appl. Phys., **67**, pp. 2665-2667, 1990.

[9]A. T. Semenov, V. R. Shidlovski, S. A. Safin, V. P. Konyaev and M. V. Zverkov, "Superluminescent diodes for visible (670 nm) spectral range based on AlGaInP/ GaInP heterostructures with tapered grounded absorber", Electron. Lett., **29**, pp. 530-531, 1993.

[10]P. L. Gourley, C. P. Tigges, R. P. Schneider, Jr., T. M. Brennan, B. E. Hammons and A. E. McDonald, "Optical properties of fractal quantum wells", Appl. Phys., Lett., **62**, pp. 1736-1738, 1993.

[11]A (room temperature) composition dependent bandgap equation for $Al_xGa_{1-x}As$ of $E_g(x) = 1.424 + 1.247x$ (eV) was assumed (H. C. Casey and M. B. Panish in *Heterostructure Lasers* (Academic, New York, 1978) pt. A p. 193. At low temperature, a GaAs bandgap of 1.515 eV is assumed (N. Shen et al, Appl., Phys., Lett, **53**, pp. 1080-1082, 1988.)

[12]W. W. Chow, M. B. Sinclair, P. L. Gourley and M. Hagerott Crawford, unpublished.

[13]H. Haug and S. W. Koch, *Quantum theory of the optical and electronic properties of semiconductors*, 2nd edition, World Scientific, Singapore (1993).

[14] A (room temperature) bandgap equation for $(Al_yGa_{1-y})_{0.5}In_{0.5}P$ of $E_g(y) = 1.900 + 0.61y$ (eV) was assumed (A. D. Prins, J. L. Sly, A. T. Meney, D. J. Dunstan, E. P. O'Reilly, A. R. Adams and A. Valster, " Band structure measurements of AlGaInP", presented at the 22nd International Conference on the Physics of Semiconductors, Vancouver, Canada, August 15-19, 1994)

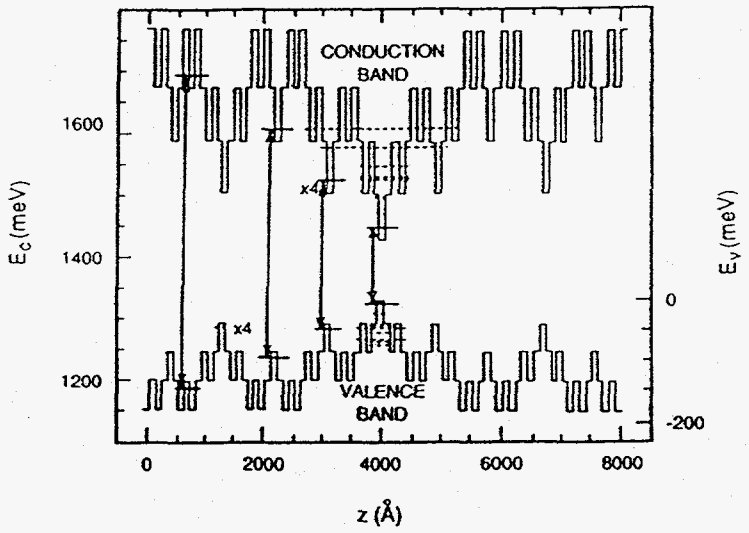

Figure 1: Schematic of the lowest energy conduction and valence bands for the 100 Å layer fractal sequence. Dominant transitions are shown by the double headed arrows.

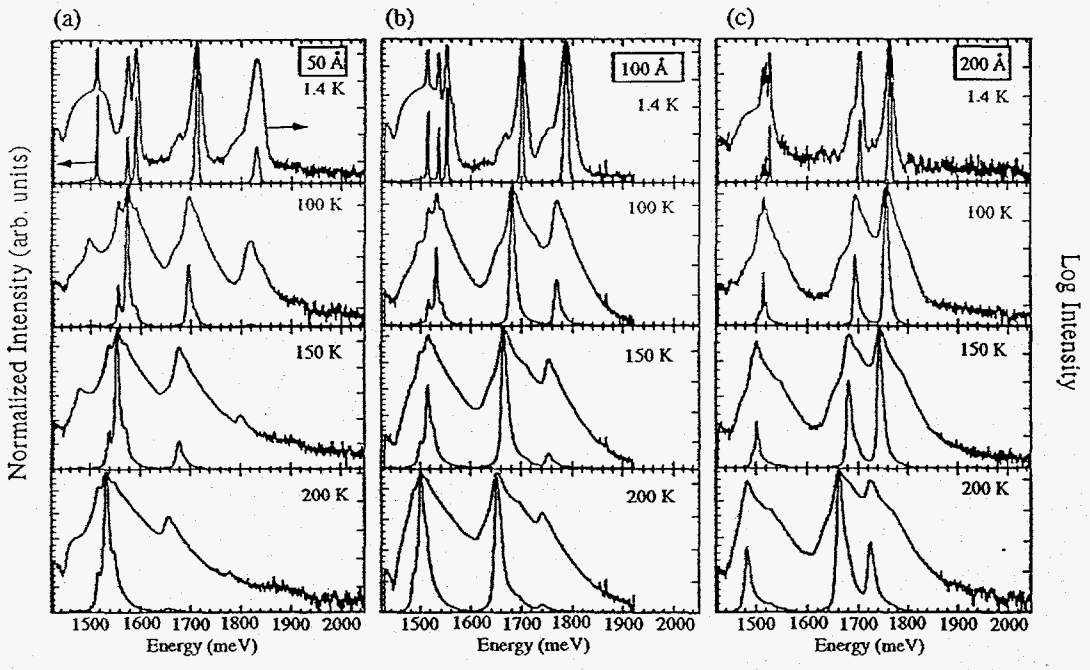

Figure 2: Temperature dependent photoluminescence and log of the photoluminescence for AlGaAs-based fractal quantum wells with characteristic layer thickness of (a) 50 Å (b) 100 Å and (c) 200 Å.

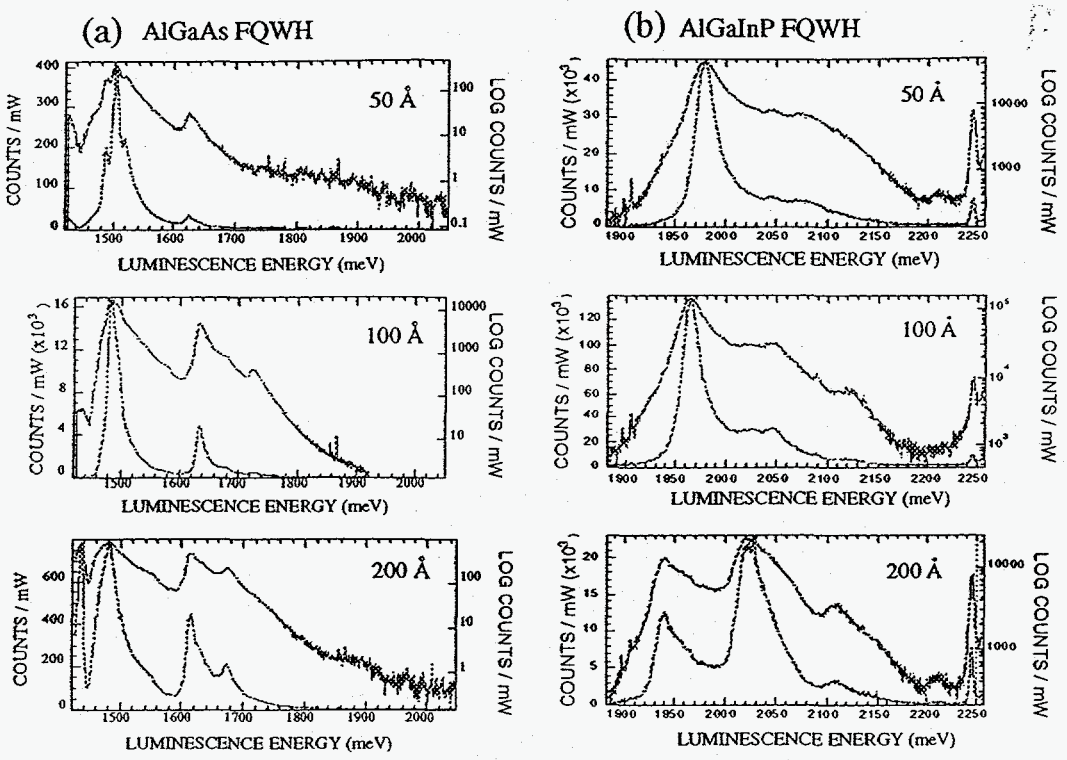

Figure 3: Room temperature photoluminescence spectra for fractal quantum wells of (a) AlGaAs alloys with 50 Å, 100 Å and 200 Å layer thickness and (b) AlGaInP alloys with 50 Å, 100 Å and 200 Å layer thickness.

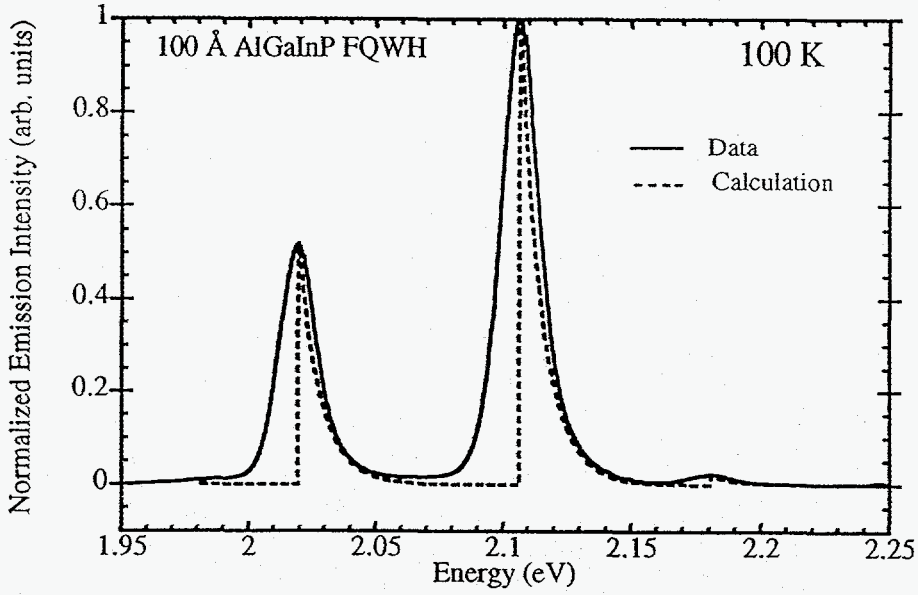

Figure 4: Normalized photoluminescence spectrum (solid curve) and calculated photoluminescence spectrum (dashed curve) of AlGaInP fractal quantum well structure with 100 Å layer thickness at 100 K.

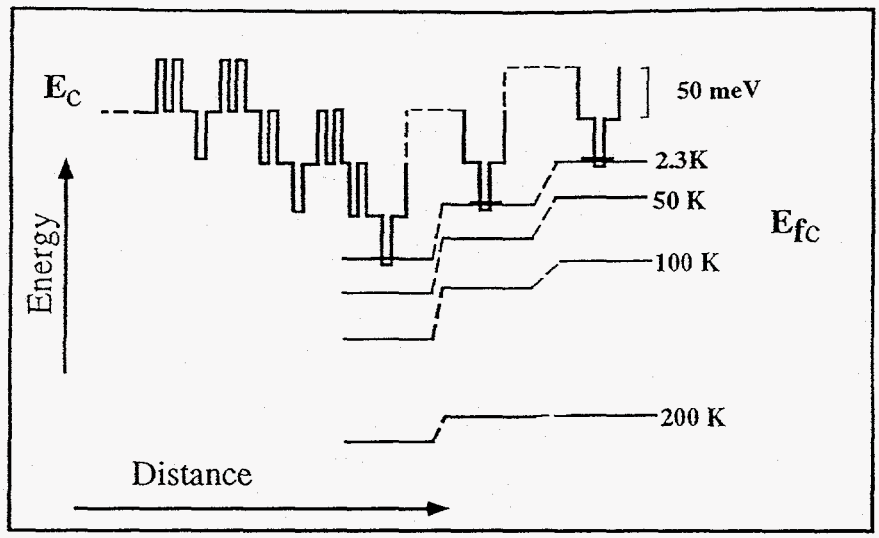

Figure 5: Schematic of the 100 Å AlGaInP fractal quantum well conduction band profile (left) and the simpler three well system considered in the calculations (right). The calculated electron effective Fermi level is shown for each of the three wells as a function of temperature.

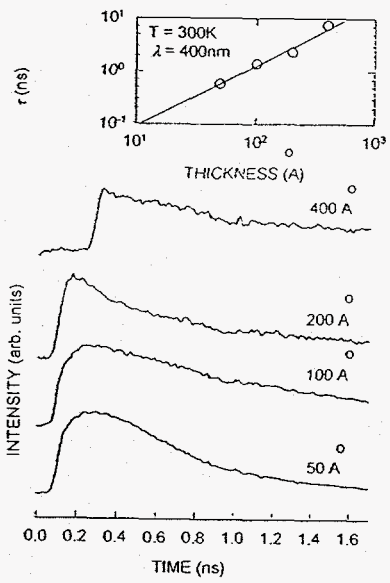

Figure 6: Room temperature time resolved photoluminescence of 50 Å, 100 Å, 200 Å and 400 Å layer thickness AlGaInP fractal quantum well structures. The inset shows the log-log plot of the photoluminescence decay time versus the characteristic layer thickness of the structure.

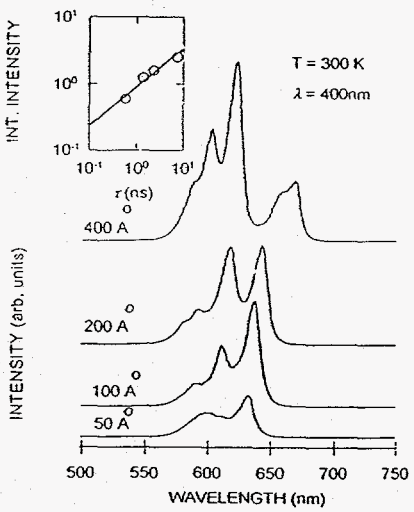

Figure 7: Emission spectrum from AlGaInP fractal quantum well heterostructures under high excitation conditions. The inset shows the log-log plot of the integrated emission intensity versus the decay time.